

NONLINEAR VIBRATION ABSORBER FOR REDUCING HAND VIBRATION FROM A VIBRO-IMPACT HAMMER MODEL

Oreoluwa Alabi

Department of Biomedical Engineering and Mechanics
Virginia Polytechnic Institute and State University
Blacksburg, Virginia 24061

Sunit Kumar Gupta, Oumar Barry*

Department of Mechanical Engineering
Virginia Polytechnic Institute and State University
Blacksburg, Virginia 24061

ABSTRACT

The transmission of vibrations from hand-held impact machines (HHIM) to the human hands is undesirable and can cause serious injury, including amputation of the hand. Therefore, it is crucial to analyze and develop efficient vibration control methods to curb vibration transmission to the hands from a HHIM. The first step towards developing an efficient vibration control method is to obtain a model that can accurately predict the dynamics of the HHIM. Thereafter, a numerical or theoretical study of the HHIM-Vibration control device model can reveal the devices effectiveness. To address the need for a HHIM model, we analyze a reduced order model of a HHIM which incorporates the vibro-impact interactions of the HHIM bit with the ground. The effectiveness of a cubic nonlinear absorber in the HHIM is then studied via a lumped mass parameter model consisting of a vibro-impact tool model coupled to the hand-arm system (HAS) and a cubic nonlinear tuned vibration absorber (NLTVA). A detailed numerical analysis of this system is performed to show the rich nonlinear dynamics of the system. The results from this study show that an appropriate selection of absorber parameters can effectively change the amplitude and periodicity of vibrations at the hand, thereby proving the potential of a cubic nonlinear absorber as a viable vibration control option.

INTRODUCTION

During the operation of heavy hand-held impact machines (HHIM) such as chipping hammers, a significant level of vibrations can be transmitted to the human hands, which can further cause injury to the hands [1]. Prolonged exposure to such vibrations may lead to episodes of vascular, musculoskeletal, and neurological disorders termed hand-arm vibration syndromes (HAVS). In extreme cases, HAVS can result in a loss of blood supply to the fingers leading to gangrene and, eventually, amputation [2]. Therefore the reduction of these vibrations transmitted to the human hand from the HHIM is essential. This is the focus of the current work. To prevent the occurrence of HAVS, it is important to have a thorough understanding of the dynamics of HHIM in order to aid the development of methods to reduce vibrations from the HAS.

One of the most widely used models in the literature to describe the dynamics of percussive tools is a lumped parameter model. A lumped parameter model is often employed due to its ability to capture the major dynamics of a system with relatively cheap computing power. Some of the models used to describe the qualitative and quantitative dynamics of percussive tools range from models described using simple visco-elastic connections to models containing cubic and nonsmooth nonlinearities, which describe the vibro-impact nature of a percussive tool operation [3–11]. Towards analyzing the qualitative dynamics of a hand-held tool, Alabi *et al.* [6, 7] studied a model of an HHIM where the dominant form of nonlinearity was considered cubic and showed the efficacy of a nonlinear absorber to

*Corresponding Author (Email: obarry@vt.edu)

reduce vibrations transmitted to the hand from such a tool. Furthermore, to manufacture vibro-impact models that could effectively describe phenomenon associated with drill-string drilling, Pavlovskaja *et al.* presented vibro-impact models that could predict the optimal static and dynamic force to obtain an optimal progression rate for drilling [4, 5]. Aguiar *et al.* showed that a 7DOF vibro-impact system could reproduce experimental relations obtained between axial vibration peaks and mud flow rate for a drilling system [3]. Franca and Weber presented a mathematical model, considering only the percussive action of a resonance hammer, and were able to capture qualitative and quantitative results similar to experimental results [12]. Despite the wide spread efficiency of vibro-impact dynamics to describe the operation of percussive tools, there have been no attempts to determine how vibrations to the hand can be mitigated while modelling the dynamics of the tool as a vibro-impact system. This study seeks to address this gap by presenting a low-order vibro-impact impact model of a chipping hammer coupled to the hand. This study also seeks to determine what method of vibration control would be most effective in reducing vibrations to the hand.

Among the existing methods to control unwanted vibrations, a tuned vibration absorber (TVA) is more popular [13]. The efficacy of TVA is already established in dynamical systems such as grass trimmers, power lines, and in the manufacturing processes including milling and boring [14–19]. However the TVA does not offer a wide vibration frequency suppression bandwidth. On the other hand, nonlinear tuned vibration absorbers (NLTVA) have been found to have a wider suppression bandwidth in comparison to the linear TVA [20, 21]. Since the operating frequency of the chipping hammer could vary during its operation (implying a broader frequency spectrum operation), an NLTVA is considered to be more effective to control vibrations from a vibro-impact chipping hammer model. Hence, a nonlinear absorber more specifically with cubic nonlinearity is explored in this work. This choice is made because the nonlinear behavior for vibro-impact systems is similar to the basic hardening system [22, 23].

Previous studies have shown that the nonlinear vibration absorber inerter (NVAI) effectively controls vibrations when the hand-arm system is coupled with a Hand-held Impact Machine (HHIM) modeled as a 1-DOF system with visco-elastic ground-tool interaction containing cubic non-linearities [6, 7]. However, the effectiveness of the NVAI has not been explored if the interaction of the HHIM and ground is modeled as a vibro-impact model. To address this gap, this study conducts a detailed nonlinear analysis to explore vibration control at the hand for a tool modeled with vibro-impact nonlinearities.

To embark on this work, a lumped parameter model is proposed to describe the HAS-HHIM-NLTVA system dynamics in the axial direction as the dominant axis of the tool considered in this study is in the axial direction [1]. A reduced order model of the percussive tool is introduced as a 2-DOF vibro-impact

lumped parameter model, while the hand-arm system is modeled as a 2-DOF parameter model. The non-smooth system is smoothed via Filippov’s method, and the system is analyzed qualitatively using nonlinear tools. The rest of the paper is organized as follows. In section 1, the mathematical model of the vibro-impact HAS-HHIM-NLTVA system is presented. In section 2, the smoothing of the non-smooth system and bifurcation analysis of the system are presented. Also, phase portraits are used to analyze the system’s dynamics. Further the significance of the results obtained is discussed in section 3. Finally, some conclusions are drawn on the study in section 4.

1 Model development of HHIM-HAS-NVAI system

In this section, we present the reduced-order vibro-impact model of the coupled HAS-HHIM-NLTVA system. The schematic of the system is shown in Fig.1. In the schematic, the bit of the HHIM is modeled as a lumped mass, m_p , whereas the housing of the HHIM is modeled as a lumped mass m_H . The parameters of the HHIM bit and casing are adopted from the model generated by Golysheva *et al.* [24] for a heavy electro-pneumatic hammer drill (Hilti TE 74) operating at 45Hz. The buffer between the HHIM bit and casing is modeled as a visco-elastic connection with parameters adopted from [24]. In this model, we account for the feed force to press the machine against the material being worked on.

To capture the HHIM dynamics associated with the percussive action of the HHIM piston on the HHIM bit, a nonlinear interaction is specified between the HHIM bit and the ground material. To do so, the ground material is modeled as a linear spring-damper as presented in [24–26] with the initial separation of g from the HHIM bit. In this model, the ground material is restored before each successive impact, and the process of penetration of material is not taken into consideration. In this work, we consider concrete as the ground material with the stiffness and loss factors adopted from [24].

Furthermore, the hand-arm system is modeled as a 2-DOF freedom system as it provides a fairly accurate response of the hand at frequencies less than 100Hz [27]. Therefore, this model will be appropriate for our system, which operates at 45Hz.

1.1 Non-smooth model

In the schematic, x_H , x_a , x_N , x_p , and y represent the motion of the HHIM casing, HAS, NVAI, HHIM bit, and massless support, respectively.

Due to the discontinuous nature of the HAS-HHIM-NLTVA system, the governing equations of motion can be defined using two different sets of differential equations. One set of equations corresponds to the scenario when the HHIM bit is not in contact with the material, while the other set of equations corresponds to the case when the bit is in contact with the material. Defining f_m

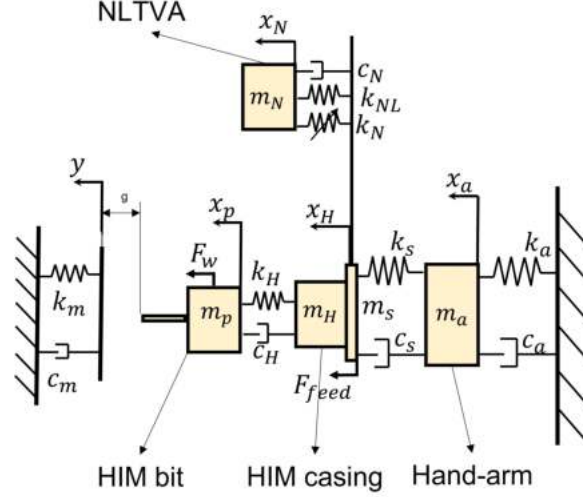


FIGURE 1: Schematic of the combined system of HHIM-HAS system with a NLTVA

as the contact force between m_p and the material, the conditions for these two different scenarios are listed below:

$$\begin{cases} x_p < g \text{ and } f_m = 0, \text{ without contact.} \\ x_p \geq g \text{ and } f_m = -(k_m y + c_m \dot{y}) < 0, \text{ with contact.} \end{cases} \quad (1)$$

Similar to the discontinuous support system presented by Leine [28], the support in the current work relaxes to the equilibrium state if the mass is not in contact with the support. While assuming that the relaxation time of the support is much smaller than the time between two contact events, the free motion of the support is neglected. With these assumptions, the governing equations of motion of the system are given:

$$\begin{aligned} (m_H + m_s) \ddot{x}_H - \dot{x}_a c_s - x_a k_s - \dot{x}_p c_H - x_p k_H - \dot{x}_N c_N - k_{NL} x_N + \\ \dot{x}_H (c_H + c_N + c_s) + x_H (k_H + k_{NL} + k_s) + \\ k_N (x_H - x_N)^3 = F_{feed}, \end{aligned} \quad (2a)$$

$$m_a \ddot{x}_a + \dot{x}_a (c_a + c_s) + x_a (k_a + k_s) - \dot{x}_H c_s - x_H k_s = 0, \quad (2b)$$

$$m_N \ddot{x}_N + c_N (\dot{x}_N - \dot{x}_H) + k_N (x_N - x_H)^3 + k_{NL} (x_N - x_H) = 0, \quad (2c)$$

$$\begin{aligned} m_p \ddot{x}_p + \dot{x}_p (c_H + c_m) + (x_p - g) k_m + x_p k_H - \dot{x}_H c_H - x_H k_H \\ = F_w \text{ (with contact),} \\ m_p \ddot{x}_p + \dot{x}_p (c_H) + x_p (k_H) - \dot{x}_H c_H - x_H k_H = F_w \text{ (without contact).} \end{aligned} \quad (2d)$$

In the above governing equations of motion, F_{feed} represents the feed force applied to the tool by an operator. F_w represents

the excitation force acting on the HHIM due to the reciprocating motion of the piston inside the HHIM. The analytical form of F_w is adapted from the experiments reported in [29] and is given by

$$F_w = F_{ref} \left(\frac{\omega}{\omega_{ref}} \right)^2 \sin(\omega t). \quad (3)$$

To obtain numerical solutions for the above discontinuous system (Eq. (2)), the system is convexified into a differential inclusion by the Filippov theory [30] before numerically simulating the system using the switch model suggested by Leine [28]. With this formulation, the state space \mathbb{R}^n is split into two subspaces \mathcal{V}_- and \mathcal{V}_+ by a hyper-surface Σ such that $\mathbb{R}^n = \mathcal{V}_- \cup \Sigma \cup \mathcal{V}_+$. The hypersurface Σ is called the switching boundary and is defined by a scalar switching boundary function $h(x)^2$. The state x is in Σ when

$$h(x) = 0 \iff x \in \Sigma.$$

The subspaces \mathcal{V}_- and \mathcal{V}_+ and switching boundary Σ can be formulated as

$$\begin{aligned} \mathcal{V}_- &= \{x \in \mathbb{R}^n \mid h(x) < 0\}, \\ \Sigma &= \{x \in \mathbb{R}^n \mid h(x) = 0\}, \\ \mathcal{V}_+ &= \{x \in \mathbb{R}^n \mid h(x) > 0\}. \end{aligned}$$

Therefore, a discontinuous differential equation can be cast

as:

$$\dot{x}(t) \in F(t, x(t)) = \begin{cases} f_-(t, x(t)), & x \in \mathcal{V}_-, \\ \overline{\text{co}}\{f_-(t, x(t)), f_+(t, x(t))\}, & x \in \Sigma \\ f_+(t, x(t)), & x \in \mathcal{V}_+ \end{cases}$$

where the convex set is defined as

$$\overline{\text{co}}\{f_-, f_+\} = \{(1-q)f_- + qf_+, \forall q \in [0, 1]\}.$$

In this system, separate conditions are required for the HHIM bit mass (m_p) to initiate contact with the support and for the bit mass to lose contact with the support. The switching boundary Σ is made up of the union of Σ_α and Σ_β . The two boundary functions for the switching boundaries are defined as:

$$\begin{aligned} h_\alpha(x_p, \dot{x}_p) &= x_p - g, \\ h_\beta(x_p, \dot{x}_p) &= k_m(x_p - g) + c_m \dot{x}_p \end{aligned} \quad (4)$$

The mass is not in contact with the support if $x \in \mathcal{V}_-$, with

$$\mathcal{V}_- = \{x \in \mathbb{R}^2 \mid h_\alpha(x_p, \dot{x}_p) < 0 \text{ or } h_\beta(x_p, \dot{x}_p) < 0\} \quad \text{no contact,}$$

and the mass is in contact with the support if $x \in \mathcal{V}_+$, with

$$\mathcal{V}_+ = \{x \in \mathbb{R}^2 \mid h_\alpha(x_p, \dot{x}_p) > 0 \text{ and } h_\beta(x_p, \dot{x}_p) > 0\} \quad \text{contact.}$$

The switching boundary Σ_α is defined by

$$\Sigma_\alpha = \{x \in \mathbb{R}^2 \mid h_\alpha(x_p, \dot{x}_p) = 0, h_\beta(x_p, \dot{x}_p) \geq 0\}.$$

The switching boundary Σ_β is defined by

$$\Sigma_\beta = \{x \in \mathbb{R}^2 \mid h_\alpha(x_p, \dot{x}_p) \geq 0, h_\beta(x_p, \dot{x}_p) = 0\}.$$

With f_+ and f_- obtained as:

$$f_+(x, t) = \begin{bmatrix} \dot{x}_H \\ \frac{1}{m_H + m_s} (\dot{x}_a c_s + x_a k_s + \dot{x}_p c_H + x_p k_H + \dot{x}_N c_N + k_{NL} x_N - \dot{x}_H (c_H + c_N + c_s) - x_H (k_H + k_{NL} + k_s) - k_N (x_H - x_N)^3 + F_{feed}) \\ \dot{x}_a \\ \frac{1}{m_a} (-\dot{x}_a (c_a + c_s) - x_a (k_a + k_s) + \dot{x}_H c_s + x_H k_s) \\ \dot{x}_N \\ \frac{1}{m_N} (-c_N (\dot{x}_N - \dot{x}_H) - k_N (x_N - x_H)^3 - k_{NL} (x_N - x_H)) \\ \dot{x}_p \\ \frac{1}{m_p} (-\dot{x}_p (c_H + c_m) - (x_p - g) k_m - x_p k_H + \dot{x}_H c_H + x_H k_H + F_w) \end{bmatrix}$$

(5)

$$f_-(x, t) = \begin{bmatrix} \dot{x}_H \\ \frac{1}{m_H + m_s} (\dot{x}_a c_s + x_a k_s + \dot{x}_p c_H + x_p k_H + \dot{x}_N c_N + k_{NL} x_N - \dot{x}_H (c_H + c_N + c_s) - x_H (k_H + k_{NL} + k_s) - k_N (x_H - x_N)^3 + F_{feed}) \\ \dot{x}_a \\ \frac{1}{m_a} (-\dot{x}_a (c_a + c_s) - x_a (k_a + k_s) + \dot{x}_H c_s + x_H k_s) \\ \dot{x}_N \\ \frac{1}{m_N} (-c_N (\dot{x}_N - \dot{x}_H) - k_N (x_N - x_H)^3 - k_{NL} (x_N - x_H)) \\ \dot{x}_p \\ \frac{1}{m_p} (-\dot{x}_p (c_H) - x_p (k_H) + \dot{x}_H c_H + x_H k_H + F_w) \end{bmatrix}$$

(6)

The numerical solutions for our system are obtained using the switch model proposed by Leine *et al.* [31]. The Switch Model introduces a band or with thickness 2η around Σ , thereby allowing the efficient numerical approximation of the system's dynamics.

2 RESULTS

In this section, the effectiveness of the nonlinear vibration absorber to control the vibrations from HHIM is explored by simulating the system's dynamics under different working conditions. For this, we use the bifurcation diagrams and corresponding phase portraits of the system. In particular, a parametric analysis is performed on the bifurcation of the system with forcing (F_{ref}) as a bifurcation parameter. Then the effect of feed force on the system's dynamics is explored using phase portraits. The parameters used in the system analysis are listed in Table 1 unless otherwise stated in the figure caption. In the first step, we perform the parametric variation of k_N .

2.1 Parametric study of K_N

We explore the effectiveness of the proposed vibration absorber through the bifurcation diagrams. For this exercise, we plot the bifurcation diagram for two different values of K_N . These bifurcation diagrams are plotted on the space of F_{ref} as the

TABLE 1: Parameter values of the HHIM-HAS-NLTVA system used for simulations.

Parameter	Value	Unit	Parameter	Value	Unit	Parameter	Value	Unit
m_H	8	kg	k_H	495020	N/m	c_H	212	Ns/m
m_a	1.55	kg	k_a	4279	N/m	c_a	76	Ns/m
m_s	0.049	kg	k_s	62804	N/m	c_s	193	Ns/m
m_N	$0.02m_H$	kg	k_{NL}	14549	N/m	c_N	9.3	Ns/m
F_{ref}	300	N	ω_{ref}	45	Hz	g	0.02	m
m_p	0.35	kg	k_N	2.5×10^6	Ns/m ³	F_{feed}	250	N
—	—	—	k_m	3×10^7	N/m	c_m	4536	Ns/m

bifurcation parameter and response of the hand x_a as the variable of interest. These bifurcation diagrams are shown in Fig. 2.

From Fig.2a, we can observe a route via period-doubling from periodic motion to aperiodic motion. A closer look at Fig.2a and b reveals that the forcing amplitude at which the period-doubling cascade begins (point A) is decreased by increasing the cubic stiffness of the absorber. When the system has no absorber, period-doubling begins at $F_{ref} = 613N$ while adding the absorber decreases this value to $F_{ref} = 532N$. Also, the excitation forcing amplitude at which the period-1 motion initially jumps down in amplitude (point B) is decreased by the addition of the absorber, i.e., at $F_{ref} = 514N$ for the system with no absorber to $F_{ref} = 431$ for the system with the absorber. Interestingly, the absorber can increase the amplitude for certain forcing parameter ranges. As shown at point C, the amplitude of the system slightly increases (by $0.3mm$) due to the addition of the NLTVA. The periodic and aperiodic motions associated with this change are highlighted by phase portraits in Fig. 3a and b. However, at $F_{ref} = 500$ (point D), the amplitude at hand can also be reduced by adding the absorber. The bifurcation diagram shows a reduction in amplitude of about $0.8mm$ for this change.

Based on these observations, it can be concluded that the periodicity and amplitude of motion at hand can be changed by adding a cubic absorber to the vibro-impact system. The investigation by bifurcation diagrams and phase portraits has shown that adding the absorber can effectively reduce the amplitude of vibrations transmitted to the hand within a certain forcing amplitude range. Next, we evaluate the effect of changing the absorbers' damping, c_N , on the system's response.

2.2 Parametric study of c_N

Similar to the analysis for K_N , bifurcation diagrams and phase portraits are used to investigate the effects of varying the absorbers damping (c_N) on the dynamics of the system. During the operation of a percussive tool such as a chipping ham-

mer, an operating region with periodic motion is often preferred to other forms of motion as the HHIM achieves more efficient metrics such as penetration rate in this region [4]. Interestingly decreasing the absorbers' damping can cause a deviation from this wanted effect, as shown via Fig. 4. We can further observe from Fig. 4a and b that the excitation amplitude value (point F), at which there is a transition from periodic to quasi-periodic/chaotic motion, decreases with a decrease in c_N . Further, point F, at which HHIM exhibits a periodic ($F_{ref} = 630$), will show aperiodic motion for the decrease value of damping. These dynamics are shown via phase portraits in Fig. 5.

From Fig. 4a and b at point E, it can be seen that decreasing the value of the absorbers damping (from $27.9Ns/m$ to $18.6Ns/m$) leads to a decrease in amplitude at the hand of about $0.1mm$. This behavior is beneficial as lower amplitude implies lower magnitudes of vibrations transferred to the hand.

As with the parametric study for k_N , a careful selection of absorber properties can ensure the absorber enhances or deteriorates the performance of the vibro-impact system in different frequency ranges. Next, the effect of feed force on the absorber's performance is evaluated.

2.3 Effect of Feedforce (F_{feed}) on absorber performance

Note that Dong *et al.* [1] observed that the feed force applied to an HHIM greatly affects the vibrations emitted by the tool. As such, the variation in vibrations at hand with a varied feed force is explored, and the absorber's effectiveness with this varied feed force is also explored.

When the feed force is lowered from 250N to 200N, a comparison between Fig. 3c and Fig. 6a reveals that the system dynamics transition from periodic to aperiodic motion. This transition from periodic to aperiodic motion also results in an increase in the vibration amplitude at the fingers of $0.1mm$. When the cubic absorber is added to the system, the amplitude increases

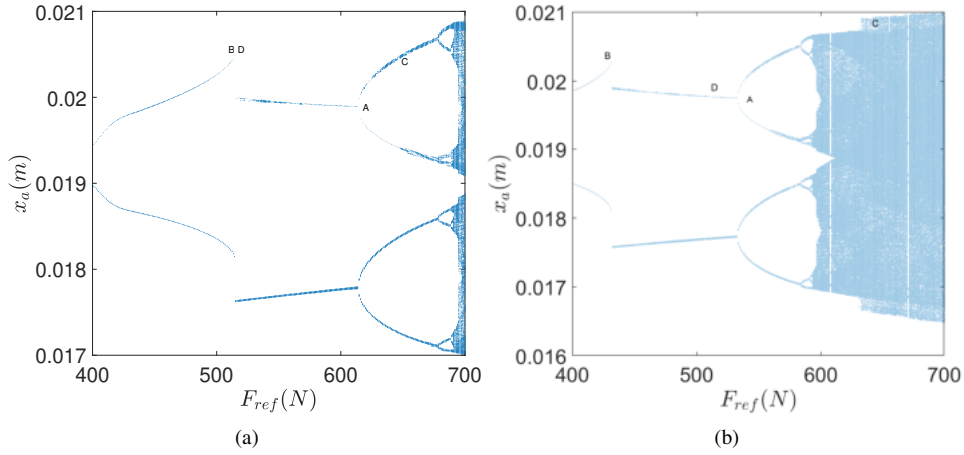


FIGURE 2: Comparison of bifurcation diagram for different values of k_N . Bifurcation diagrams for $\omega = 47\text{Hz}$ and $k_N =$ a) 0, b) 2.5×10^6 .

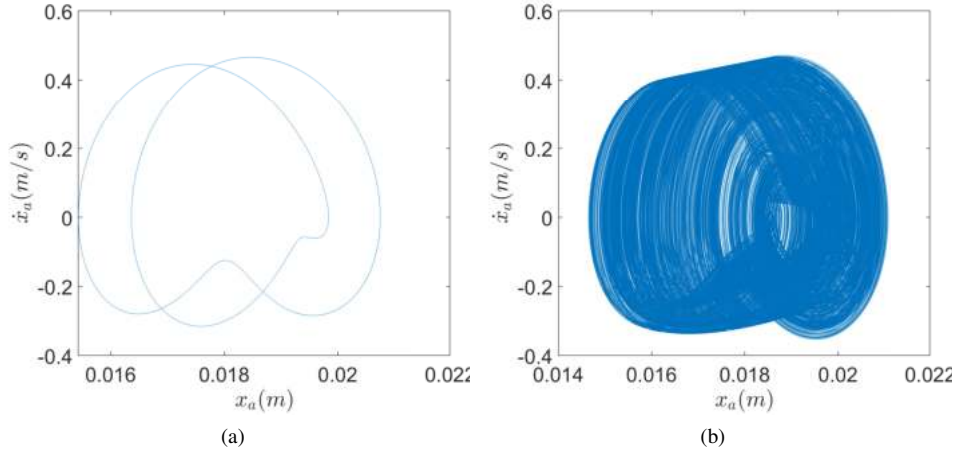


FIGURE 3: Comparison of phase portrait for different values of k_N . Phase portrait for $\omega = 47\text{Hz}$, $F_{ref} = 650$ and $k_N =$ a) 0N/m , b) $2.5 \times 10^6\text{N/m}$ and $F_{ref} = 500\text{N}$, $k_N =$ c) 0N/m , d) $2.5 \times 10^6\text{N/m}$

by 0.1mm . This result is in opposition to the result found for $F_{feed} = 250\text{N}$ where the addition of the absorber improved and reduced the vibration amplitude at the fingers. This result implies the need to carefully tune the absorber based on the feed force being applied to the system.

3 DISCUSSION

The implication of the results based on the above parametric study performed is that the performance of the absorber varies and depends on the forcing range in which the vibro-impact system operates. This preliminary exploration leads to the conclusion that for the absorber to be effective, it must be tuned based

on the forcing range within which the HHIM operates. It is worth noting that a percussive tool such as the chipping hammer operates most efficiently when in the periodic regime. The NLTVA above has been found to be effective in reducing the vibration at hand in this regime.

This investigation also revealed how the feed force could significantly change the system's dynamic from periodic to aperiodic and amplify the vibrations at hand. Also, the vibration-dampening effect of the NLTVA was found to change when the feed force of the system was changed. This observation implies that the parameters of the NLTVA need to be properly selected based on the working feed force of the HHIM being used.

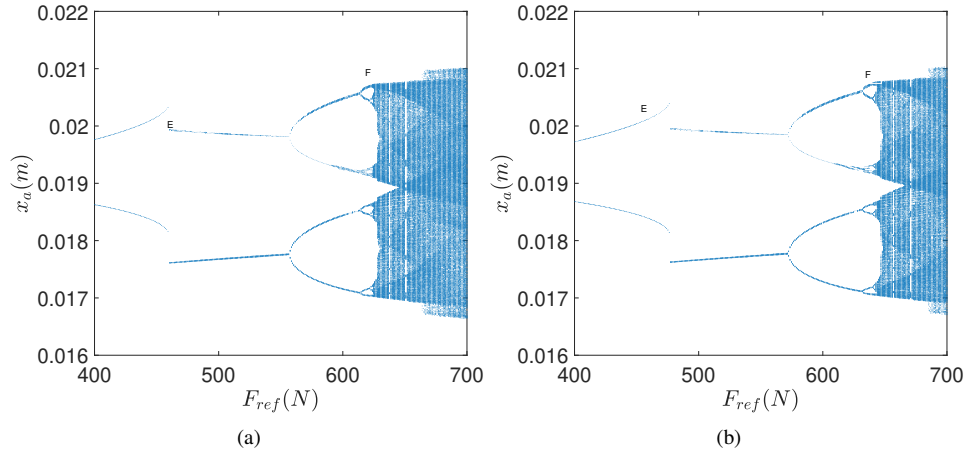


FIGURE 4: Comparison of bifurcation diagram for different values of c_N . Bifurcation diagrams for $\omega = 47$, and $c_N =$ a) $18.6 \frac{Ns}{m}$, b) $27.9 \frac{Ns}{m}$.

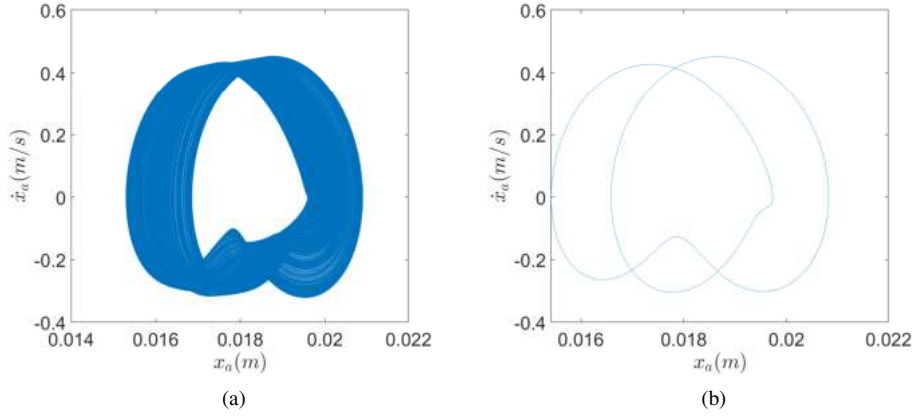


FIGURE 5: Comparison of Phase portraits for different values of c_N . Phase portrait for $\omega = 47Hz$, $F_{ref} = 630N$ and $c_N =$ a) $18.6 \frac{Ns}{m}$ and b) $27.9 \frac{Ns}{m}$.

4 CONCLUSION

We studied the effectiveness of a nonlinear tuned vibration absorber to control the vibrations transmitted to the hand from hand-held power tools more specifically a chipping hammer. We modeled the chipping hammer as a vibro-impact model to incorporate realising working conditions. The effectiveness of a nonlinear absorber was explored through a parametric analysis based on the bifurcation of the system. For this we choose the absorber's stiffness, damping and feed force as our primary parameters. This analysis revealed that the absorber could reduce or amplify hand vibrations based on the excitation forcing range of the HHIM. This undesired amplification was found when a transition occurred from periodic to aperiodic motion. However, it was seen that when the HHIM operates efficiently in a periodic

regime, the absorber is able to reduce vibrations at hand. Further, a parametric analysis of the feed force applied at the system showed that the absorber would need to be retuned if the feed force applied on the HHIM changes. These results prove the potential of a cubic absorber as a viable vibration control option for the HHIM. These results also prove the need to optimize the parameters of the cubic absorber so it is always effective for a selected HHIM system.

REFERENCES

- [1] Dong, R., McDowell, T., Welcome, D., Warren, C., and Schopper, A., 2004. "An evaluation of the standardized chipping hammer test specified in iso 8662-2". *Annals of*

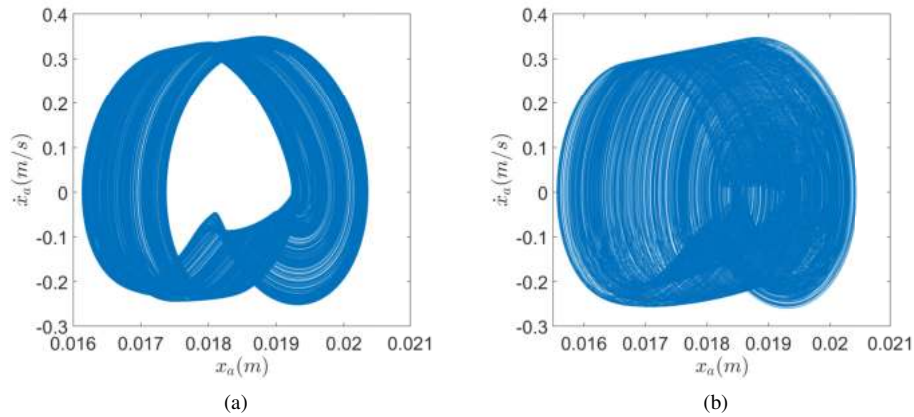


FIGURE 6: Comparison of Phase portraits for $F_{feed} = 200N$ and different values of k_N . Phase portrait for $\omega = 47Hz$, $F_{ref} = 500N$ and $k_N =$ a) $0N/m$ and b) $2.5 \times 10^6 N/m$.

- occupational hygiene*, **48**(1), pp. 39–49.
- [2] Welcome, D. E., Dong, R. G., Xu, X. S., Warren, C., and McDowell, T. W., 2014. “The effects of vibration-reducing gloves on finger vibration”. *International journal of industrial ergonomics*, **44**(1), pp. 45–59.
- [3] Aguiar, R., d’Almeida, E., and Ritto, T., 2020. “Vibro-impact model and validation of the axial dynamics of a vibration-assisted drilling tool”. *Journal of the Brazilian Society of Mechanical Sciences and Engineering*, **42**, pp. 1–16.
- [4] Pavlovskaja, E., Hendry, D. C., and Wiercigroch, M., 2015. “Modelling of high frequency vibro-impact drilling”. *International Journal of Mechanical Sciences*, **91**, pp. 110–119.
- [5] Pavlovskaja, E., Wiercigroch, M., and Grebogi, C., 2001. “Modeling of an impact system with a drift”. *Physical Review E*, **64**(5), p. 056224.
- [6] Alabi, O., Gupta, S. K., and Barry, O., 2022. “Dynamics of a nonlinear absorber and hand-held impact machine”. In *International Design Engineering Technical Conferences and Computers and Information in Engineering Conference*, Vol. 86304, American Society of Mechanical Engineers, p. V009T09A022.
- [7] Alabi, O., Gupta, S. K., and Barry, O., 2023. “Vibration analysis of a nonlinear absorber coupled to a hand-held impact machine”. *Journal of Computational and Nonlinear Dynamics*, pp. 1–18.
- [8] Wiercigroch, M., and Pavlovskaja, E., 2003. “Nonlinear dynamics of vibro-impact systems: theory and experiments”. In *Materials science forum*, Vol. 440, Trans Tech Publ, pp. 513–520.
- [9] Cao, Q.-J., Wiercigroch, M., Pavlovskaja, E., and Yang, S.-P., 2010. “Bifurcations and the penetrating rate analysis of a model for percussive drilling”. *Acta Mechanica Sinica*, **26**(3), pp. 467–475.
- [10] Wiercigroch, M., 2006. “Applied nonlinear dynamics of non-smooth mechanical systems”. *Journal of the Brazilian Society of Mechanical Sciences and Engineering*, **28**(4), pp. 519–526.
- [11] Ho, J.-H., Nguyen, V.-D., and Woo, K.-C., 2011. “Nonlinear dynamics of a new electro-vibro-impact system”. *Nonlinear dynamics*, **63**(1), pp. 35–49.
- [12] Franca, L. F. P., and Weber, H. I., 2004. “Experimental and numerical study of a new resonance hammer drilling model with drift”. *Chaos, Solitons & Fractals*, **21**(4), pp. 789–801.
- [13] Frahm, H., 1911. Device for damping vibrations of bodies., Apr. 18. US Patent 989,958.
- [14] Hao, K. Y., and Ripin, Z. M., 2013. “Nodal control of grass trimmer handle vibration”. *International Journal of Industrial Ergonomics*, **43**(1), pp. 18–30.
- [15] Liu, W., Dai, H., and Wang, L., 2017. “Suppressing wind-induced oscillations of prismatic structures by dynamic vibration absorbers”. *International Journal of Structural Stability and Dynamics*, **17**(06), p. 1750056.
- [16] Barry, O., and Bukhari, M., 2017. “On the modeling and analysis of an energy harvester moving vibration absorber for power lines”. In *Dynamic Systems and Control Conference*, Vol. 58288, American Society of Mechanical Engineers, p. V002T23A005.
- [17] Febbo, M., 2012. “Optimal parameters and characteristics of a three degree of freedom dynamic vibration absorber”. *Journal of vibration and acoustics*, **134**(2).
- [18] Shakeri, S., and Samani, F. S., 2017. “Application of linear and nonlinear vibration absorbers in micro-milling process in order to suppress regenerative chatter”. *Nonlinear Dynamics*, **89**(2), pp. 851–862.

- [19] Moradi, H., Bakhtiari-Nejad, F., and Movahhedy, M., 2008. “Tuneable vibration absorber design to suppress vibrations: an application in boring manufacturing process”. *Journal of Sound and Vibration*, **318**(1-2), pp. 93–108.
- [20] Lacarbonara, W., and Cetraro, M., 2011. “Flutter control of a lifting surface via visco-hysteretic vibration absorbers”. *International Journal of Aeronautical and Space Sciences*, **12**(4), pp. 331–345.
- [21] Poovarodom, N., Kanchanosot, S., and Warnitchai, P., 2003. “Application of non-linear multiple tuned mass dampers to suppress man-induced vibrations of a pedestrian bridge”. *Earthquake engineering & structural dynamics*, **32**(7), pp. 1117–1131.
- [22] Babitsky, V. I., 2013. *Theory of vibro-impact systems and applications*. Springer Science & Business Media.
- [23] Habib, G., Detroux, T., Vigiú, R., and Kerschen, G., 2015. “Nonlinear generalization of den hartog’s equal-peak method”. *Mechanical Systems and Signal Processing*, **52**, pp. 17–28.
- [24] Golysheva, E., Babitsky, V., and Veprik, A., 2004. “Vibration protection for an operator of a hand-held percussion machine”. *Journal of Sound and Vibration*, **274**(1-2), pp. 351–367.
- [25] Wiercigroch, M., Neilson, R., and Player, M., 1999. “Material removal rate prediction for ultrasonic drilling of hard materials using an impact oscillator approach”. *Physics Letters A*, **259**(2), pp. 91–96.
- [26] Wiercigroch, M., Wojewoda, J., and Krivtsov, A., 2005. “Dynamics of ultrasonic percussive drilling of hard rocks”. *Journal of Sound and Vibration*, **280**(3-5), pp. 739–757.
- [27] Dong, R. G., Welcome, D. E., Wu, J. Z., and McDowell, T. W., 2008. “Development of hand-arm system models for vibrating tool analysis and test rig construction”. *Noise Control Engineering Journal*, **56**(1), pp. 35–44.
- [28] Leine, R. I., Van Campen, D., and Van de Vrande, B., 2000. “Bifurcations in nonlinear discontinuous systems”. *Nonlinear dynamics*, **23**, pp. 105–164.
- [29] Josefsson, M., and Grétarsson, S. L., 2015. “Optimisation of a non-linear tuned vibration absorber in a hand-held impact machine”. Master’s thesis.
- [30] Filippov, A. F., 2013. *Differential equations with discontinuous righthand sides: control systems*, Vol. 18. Springer Science & Business Media.
- [31] Leine, R. I., and Nijmeijer, H., 2013. *Dynamics and bifurcations of non-smooth mechanical systems*, Vol. 18. Springer Science & Business Media.